PERGAMON

International Journal of Heat and Mass Transfer 41 (1998) 3265–3278

International Journal of
HEAT and MASS
TRANSFER

Computation of the solidification of pure metals in plate geometry using the Green's function method

Hong Sha, Klaus Schwerdtfeger*

Institut für Allgemeine Metallurgie, Technische Universität Clausthal, 38678 Clausthal-Zellerfeld, Germany

Received 28 August 1996; in final form 18 December 1997

Abstract

In this study the Green's function technique has been used to solve the solidification problem in plate geometry for three alternative types of boundary condition at the surface of the plate. With this method the differential equation for heat conduction is transformed into an integral equation with line integrals, reducing in this manner the integration to a solution at the boundaries of the domain. The advantage is a considerable saving of computer time. Simple forms of boundary condition, that is constant values of temperature T_0, of heat flux density q_0, or of heat transfer coefficient h, are used, but the treatment can readily be extended to time dependent values. The rate laws for the advancement of the solidification front and for the evolution of surface temperature (in the case of prescribed q_0 or h) are obtained and are presented in non-dimensional form. © 1998 Elsevier Science Ltd. All rights reserved.

Nomenclature

a	thermal diffusivity
Bi	Biot number
c_p	specific heat of solid
G	Green's function
h	heat transfer coefficient
L	half-width of the slab
n	number specifying node on time scale
p	dimensionless time (Fourier number)
p_E	dimensionless time to the end of solidification ($=at_E/L^2$)
Ph	phase transformation number
q_0	heat flux density
s	dimensionless coordinate
S	dimensionless shell thickness
t	time
t_E	time to the end of solidification
T	temperature
T_0	surface temperature
T_f	melting temperature of metal
T_w	reference temperature
U	dimensionless temperature
U_0	dimensionless surface temperature
x	spatial coordinate
x_s	shell thickness.

Greek symbols

δ	a small positive value
ΔH_f	heat of fusion of metal per mass unit
ε	a small positive value
η_s	rate constant in Neumann's solution
λ	heat conductivity
ξ	dimensionless coordinate at which heat source is liberated at $p = \tau$
ρ	density
τ	dimensionless time at which heat source is liberated at $s = \xi$.

Subscripts

I, II, III	type of boundary condition.

1. Introduction

The solidification rate of metals depends on various parameters. Its knowledge is frequently required for the control of solidification processes in the metallurgical industries. The mathematical problem is that of heat flow with moving phase boundary. Analytically, such a problem can be solved only for the one-dimensional Cartesian

---

* Corresponding author.

PII: S0017-9310(98)00032-5

case using the boundary condition of constant surface temperature (Neumann's solution). For other boundary conditions and other geometries (cylinder, sphere) solutions can be obtained only by numerical computation. Chuang et al. [1–5] have shown that heat conduction and mass diffusion problems involving moving phase boundaries can be solved successfully applying the Green's function method. With this method the differential equation for heat conduction (or diffusion) is transformed into an integral equation with line integrals, reducing in this manner the integration to a solution at the boundaries of the domain. The advantage is a considerable saving of computer time. Although the Green's function method is well known [6], from the general point of view, its application to moving boundary problems is not frequent [1–5, 7–10].

In the present study the Green's function technique is applied to solve the solidification problem in plate geometry for three alternative types of boundary condition at the surface of the plate. Simple forms of boundary condition (constant values of T_0, q_0, or h) are used, but the treatment can readily be extended to time dependent boundary conditions. The obtained results which are presented in non-dimensional form, can serve to predict solidification rates of pure metals (and pure compounds) and, in an approximate manner, also of alloys with small freezing range.

2. Solidification model and starting equations

The geometry of the solidifying material is that of a plate with half-thickness L, Fig. 1. Initially, there is only melt with its temperature at the solidification temperature (melting point) T_f.* The heat is withdrawn at the surface $x = 0$ of the plate causing the formation of a solid layer. The thickness of this solid shell is x_s. It is the objective of the work to compute the rate law of growth of the shell for three different types of boundary condition at the surface $x = 0$.

The extension of the plate in the two other directions (y and z) is taken to be infinite. Hence, the problem is one-dimensional and the heat flow equation to be integrated over the solid shell (material properties are set constant) is

$$\frac{\partial T}{\partial t} = a\frac{\partial^2 T}{\partial x^2} \tag{1}$$

with $a = \lambda/\rho c_p$. The initial condition is

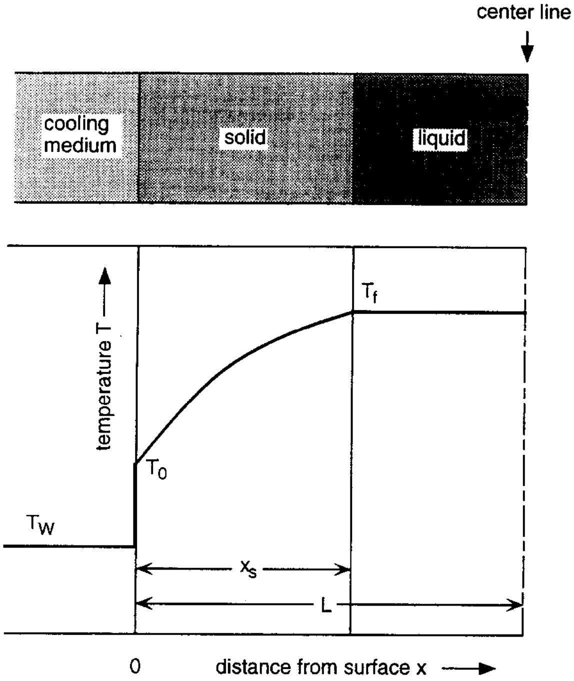

Fig. 1. Geometry of the solidifying plate and temperature profile.

$$t = 0, \quad T = T_f, \quad x_s = 0. \tag{2}$$

At the solid/liquid interface, $x = x_s$, the temperature is fixed at $T = T_f$ and the enthalpy of solidification (enthalpy of fusion) which is released due to the growth of x_s, has to be removed. Hence, there are two boundary conditions

$$x = x_s, \quad T = T_f \tag{3}$$

$$\lambda\frac{\partial T}{\partial x} = \rho \Delta H_f \frac{\mathrm{d}x_s}{\mathrm{d}t}. \tag{4}$$

At the surface of the plate, $x = 0$, three boundary conditions can be used, alternatively, depending on what is known in the particular situation.

Boundary condition at x = 0 *of the first kind*: The temperature T_0 is specified which in reality varies with time. Here, only the case of constant T_0 is treated. Hence, the boundary condition of the first kind is

$$x = 0, \quad T = T_0. \tag{5a}$$

Boundary condition at x = 0 *of the second kind*: Alternatively, the heat flux density q_0 at the surface may be known, e.g. from the increase of the cooling water temperature in a continuous casting mold. Here, we treat the case of constant heat flux density. Hence, the boundary condition of the second kind is

$$x = 0, \quad \lambda\frac{\partial T}{\partial x} = q_0. \tag{5b}$$

Boundary condition at x = 0 *of the third kind*: Neither the

---

* In practical solidification processesses, e.g. continuous casting of steel, the superheat (increase of bulk temperature of the melt over T_f) is usually very small and disappears fast, due to the convection in the melt, and, consequently, it can be neglected in many cases.

temperature nor the heat flux density at the surface may be specified, but a heat transfer coefficient h is known. We treat the case of constant h. Hence, the boundary condition of the third kind is

$$x = 0,\ \lambda\frac{\partial T}{\partial x} = h(T - T_w). \tag{5c}$$

T_w is a reference temperature, e.g. that of the water emerging from the cooling nozzles in the secondary cooling zone in continuous casting.

3. Non-dimensional formulation of the problem

The differential equation (1) together with the initial condition (2) and the boundary conditions (3), (4), and one of (5a)–(5c) represent the complete description of the mathematical problem. In order to obtain generalized results the solution is carried out in non-dimensional form. The non-dimensional variables partially differ in the treatments of the three kinds of boundary condition at $x = 0$.

Boundary condition at x = 0 *of the first kind*: The dimensionless temperature U, time p, local coordinate s, and shell thickness S are chosen as follows

$$U = \frac{T - T_0}{T_f - T_0} \tag{6}$$

$$p = \frac{at}{L^2} \tag{7}$$

$$s = \frac{x}{L} \tag{8}$$

$$S = \frac{x_s}{L}. \tag{9}$$

Using equations (6)–(9) the differential equation (1) is transformed to

$$\frac{\partial U}{\partial p} = \frac{\partial^2 U}{\partial s^2} \tag{10}$$

and the initial and boundary conditions (2), (5a), (3), (4) to

$$p = 0,\quad U = 1,\quad S = 0 \tag{11}$$

$$s = 0,\quad U = 0 \tag{12}$$

$$s = S,\quad U = 1 \tag{13}$$

$$\frac{\partial U}{\partial s} = Ph_{\mathrm{I}}\frac{\mathrm{d}S}{\mathrm{d}p}. \tag{14}$$

The 'phase transformation number' Ph_{I} is given as

$$Ph_{\mathrm{I}} = \frac{\Delta H_f}{c_p(T_f - T_0)}. \tag{15}$$

For the boundary condition of the first kind the rate law $S(p)$ is the 'square root law' $S = 2\eta_s\sqrt{p}$ with the 'rate constant' η_s depending only on Ph_{I}. The results obtained with the Green's function method can be checked with the well known Neumann's analytical solution [6].

Boundary condition at x = 0 *of the second kind*: The non-dimensional variables p, s, S are the same as for the boundary condition of the first kind, equations (7)–(9), but the non-dimensional temperature U is defined in a different manner

$$U = \frac{\lambda(T - T_f)}{q_0 L}. \tag{16}$$

The differential heat flow equation is identical to that for the boundary condition of the first kind, equation (10), but the initial and boundary conditions, corresponding to (2), (5b), (3), (4), are

$$p = 0,\quad U = 0,\quad S = 0 \tag{17}$$

$$s = 0,\quad \frac{\partial U}{\partial s} = 1 \tag{18}$$

$$s = S,\quad U = 0 \tag{19}$$

$$\frac{\partial U}{\partial s} = Ph_{\mathrm{II}}\frac{\mathrm{d}S}{\mathrm{d}p} \tag{20}$$

with the 'phase transformation number' Ph_{II} being

$$Ph_{\mathrm{II}} = \frac{\Delta H_f \lambda}{c_p q_0 L}. \tag{21}$$

The boundary condition (18) at $s = 0$ is non-homogeneous in contrast to the boundary condition of the first kind, equation (12). Again, the growth rate $S(p)$ depends on only one non-dimensional parameter Ph_{II}.

Boundary condition at x = 0 *of the third kind*: The non-dimensional variables p, s, S are again the same as for the boundary condition of the first kind and are given by equations (7)–(9), but the reference temperature T_w is used in the non-dimensional temperature U instead of the surface temperature. Hence, U is

$$U = \frac{T - T_w}{T_f - T_w}. \tag{22}$$

The differential equation is the same as before, equation (10).

The initial and boundary conditions corresponding to (2), (5c), (3), (4) are

$$p = 0,\quad U = 1,\quad S = 0 \tag{23}$$

$$s = 0,\quad \frac{\partial U}{\partial s} = Bi\,U \tag{24}$$

$$s = S,\quad U = 1 \tag{25}$$

$$\frac{\partial U}{\partial s} = Ph_{\mathrm{II}}\frac{\mathrm{d}S}{\mathrm{d}p} \tag{26}$$

with the 'phase transformation number' Ph_{III} and the Biot number Bi being

$$Ph_{\mathrm{III}} = \frac{\Delta H_f}{c_p(T_f - T_w)} \tag{27}$$

$$Bi = \frac{hL}{\lambda}. \tag{28}$$

For the boundary condition of the third kind two independent non-dimensional numbers Ph_{III} and Bi are necessary to describe the growth law $S(p)$.

4. Green's function method

The Green's functions $G(s, p, \xi, \tau)$ are solutions for the differential equation

$$\frac{\partial G}{\partial p} = \frac{\partial^2 G}{\partial s^2} \quad \text{for} \quad p > \tau \tag{29}$$

and can be taken to be the dimensionless temperature at the location s and time p due to instantaneous heat sources released at the locations ξ (and $-\xi$) and at time τ and are chosen, for the present problems, in such a manner to fulfill, in terms of G, the boundary conditions for U at $s = 0$. The following functions are available from the literature, for the three different boundary conditions used.

Boundary condition at s = 0 *of the first kind*:

$$s = 0, \quad p > \tau, \quad G = 0$$

$$G = \frac{1}{2\sqrt{\pi(p-\tau)}}\left[e^{-\frac{(s-\xi)^2}{4(p-\tau)}} - e^{-\frac{(s+\xi)^2}{4(p-\tau)}}\right]. \tag{30}$$

Boundary condition at s = 0 *of the second kind*:

$$s = 0, \quad p > \tau, \quad \frac{\partial G}{\partial s} = 0$$

$$G = \frac{1}{2\sqrt{\pi(p-\tau)}}\left[e^{-\frac{(s-\xi)^2}{4(p-\tau)}} + e^{-\frac{(s+\xi)^2}{4(p-\tau)}}\right]. \tag{31}$$

Boundary condition at s = 0 *of the third kind*:

$$s = 0, \quad p > \tau, \quad \frac{\partial G}{\partial s} = Bi\, G$$

$$G = \frac{1}{2\sqrt{\pi(p-\tau)}}\left[e^{-\frac{(s-\xi)^2}{4(p-\tau)}} + e^{-\frac{(s+\xi)^2}{4(p-\tau)}}\right] - Bi\, e^{Bi^2(p-\tau) + Bi(s+\xi)}\operatorname{erfc}\left[\frac{s+\xi}{2\sqrt{p-\tau}} + Bi\sqrt{p-\tau}\right]. \tag{32}$$

The Green's function contain the times as $p-\tau$. Hence they fulfill also the differential equation

$$\frac{\partial G}{\partial \tau} = -\frac{\partial^2 G}{\partial \xi^2} \quad \text{for}\, p > \tau. \tag{33}$$

The heat flow equation (10) can be written, using the variables ξ, τ, as

$$\frac{\partial U}{\partial \tau} = \frac{\partial^2 U}{\partial \xi^2}. \tag{34}$$

Equations (33) and (34) are now multiplied with U and G, respectively. The resulting expressions are added and an integration is performed over ξ in the range 0 to $S(p)$ and over τ in the range 0 to p. In order to avoid the singularity at $\tau = p$, the upper integration limit of τ is set $p-\varepsilon$ with ε being a positive number infinitely close to zero

$$\int_0^{p-\varepsilon}\int_0^S \left(U\frac{\partial G}{\partial \tau} + G\frac{\partial U}{\partial \tau}\right)\mathrm{d}\xi\,\mathrm{d}\tau = -\int_0^{p-\varepsilon}\int_0^S \left(U\frac{\partial^2 G}{\partial \xi^2} - G\frac{\partial^2 U}{\partial \xi^2}\right)\mathrm{d}\xi\,\mathrm{d}\tau. \tag{35}$$

The integrands on the LHS and RHS of (35) can be written as

$$U\frac{\partial G}{\partial \tau} + G\frac{\partial U}{\partial \tau} = \frac{\partial(UG)}{\partial \tau} \tag{36a}$$

$$U\frac{\partial^2 G}{\partial \xi^2} - G\frac{\partial^2 U}{\partial \xi^2} = \frac{\partial}{\partial \xi}\left(U\frac{\partial G}{\partial \xi} - G\frac{\partial U}{\partial \xi}\right). \tag{36b}$$

By application of the Gauss sentence equation (35) can be converted into an equation involving line integrals

$$\int_R (UG)\,\mathrm{d}\xi = \int_R \left(U\frac{\partial G}{\partial \xi} - G\frac{\partial U}{\partial \xi}\right)\mathrm{d}\tau \tag{37}$$

which has to be integrated along the closed line circuit shown in Fig. 2. The resulting expression is

$$\int_0^S (UG)_{\tau=p(\xi)}\,\mathrm{d}\xi - \int_0^S (UG)_{\tau=p-\varepsilon}\,\mathrm{d}\xi - \int_0^{p-\varepsilon}\left(U\frac{\partial G}{\partial \xi} - G\frac{\partial U}{\partial \xi}\right)_{\xi=S(\tau)}\mathrm{d}\tau + \int_0^{p-\varepsilon}\left(U\frac{\partial G}{\partial \xi} - G\frac{\partial U}{\partial \xi}\right)_{\xi=0}\mathrm{d}\tau = 0. \tag{38}$$

Taking the limit for ε → 0 and using

$$\lim_{\varepsilon\to 0}\int_0^S (UG)_{\tau=p-\varepsilon}\,\mathrm{d}\xi = \begin{cases} U(s,p) & \text{for}\, s < S \\ \frac{1}{2}U(s,p) & \text{for}\, s = S \end{cases} \tag{39}$$

the expressions

$$U(s,p) = \int_0^S (UG)_{\tau=p(\xi)}\,\mathrm{d}\xi - \lim_{\varepsilon\to 0}\left[\int_0^{p-\varepsilon}\left(U\frac{\partial G}{\partial \xi} - G\frac{\partial U}{\partial \xi}\right)_{\xi=S(\tau)}\mathrm{d}\tau + \int_0^{p-\varepsilon}\left(U\frac{\partial G}{\partial \xi} - G\frac{\partial U}{\partial \xi}\right)_{\xi=0}\mathrm{d}\tau\right] \quad \text{for}\, s < S \tag{40a}$$

$$\frac{1}{2}U(S,p) = \int_0^S (UG)_{\tau=p(\xi)}\,\mathrm{d}\xi - \lim_{\varepsilon\to 0}\left[\int_0^{p-\varepsilon}\left(U\frac{\partial G}{\partial \xi} - G\frac{\partial U}{\partial \xi}\right)_{\xi=S(\tau)}\mathrm{d}\tau\right.$$

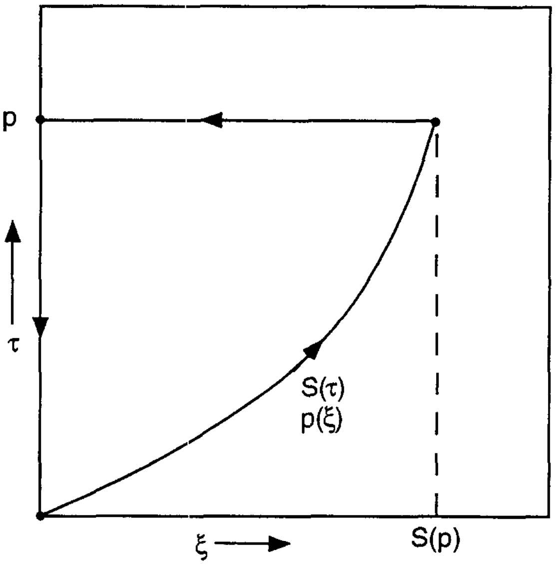

Fig. 2. Line circuit over which the line integrals in equation (37) have to be integrated.

$$+\int_0^{p-\varepsilon}\left(U\frac{\partial G}{\partial \xi}-G\frac{\partial U}{\partial \xi}\right)_{\xi=0}\mathrm{d}\tau\Bigg] \quad \text{for } s = S \qquad (40\text{b})$$

are obtained. Equation (40a) has the meaning that the temperature in the interior of the solid phase can be calculated from the temperatures and temperature gradients at the boundaries $s = 0$, $s = S$. The mathematical problem is thus reduced to a problem at the boundaries causing the savings in computer time. Equation (40b) is the starting equation for determining the rate law $S(p)$ of the growth of the shell. But instead of using (40b), the growth law $S(p)$ can be derived also by applying equation (40a) at a point $s = S-\delta$, infinitely close to $s = S$.

Solution procedure: The specific equation for three different kinds of boundary condition at $s = 0$, resulting from (40a) and (40b), are obtained by inserting the boundary conditions for U at $s = 0$ and $s = S$, and for G at $s = 0$. The solution is carried out numerically.

Boundary condition at s = 0 *of the first kind*: With $U = 1$ at $s = S$ the first integral at the RHS's of (40a) and (40b) can be transformed to

$$\int_0^S (UG)_{\tau=p(\xi)}\,\mathrm{d}\xi = \int_0^p \left(G\frac{\mathrm{d}S}{\mathrm{d}p}\right)_{\xi=S(\tau)}\mathrm{d}\tau \qquad (41)$$

and equations (42a) and (42b) become

$$U(s,p) = \lim_{\varepsilon\to 0}\Bigg[(1+Ph_{\mathrm{I}})\int_0^{p-\varepsilon}\left(G\frac{\mathrm{d}S}{\mathrm{d}p}\right)_{\xi=S(\tau)}\mathrm{d}\tau - \int_0^{p-\varepsilon}\frac{\partial G}{\partial \xi}_{\xi=S(\tau)}\,\mathrm{d}\tau\Bigg] \quad \text{for } s < S \qquad (42\text{a})$$

$$\frac{1}{2} = \lim_{\varepsilon\to 0}\Bigg[(1+Ph_{\mathrm{I}})\int_0^{p-\varepsilon}\left(G\frac{\mathrm{d}S}{\mathrm{d}p}\right)_{\xi=S(\tau)}\mathrm{d}\tau - \int_0^{p-\varepsilon}\frac{\partial G}{\partial \xi}_{\xi=S(\tau)}\,\mathrm{d}\tau\Bigg] \quad \text{for } s = S. \qquad (42\text{b})$$

The $S(p)$ relation is made discrete by dividing p and S in intervals $p_0, p_1, \ldots, p_{n-1}, p_n, \ldots, p_N$ and $S_0, S_1, \ldots, S_{n-1}, S_n, \ldots, S_N$ with $p_0 = 0$, $S_0 = 0$ and $p_N = p-\varepsilon$ and $S_N = S(p-\varepsilon)$. Within each interval the solidification rate $\mathrm{d}S/\mathrm{d}p$ is taken to be constant. Hence, the integration of the integrals can be performed analytically for each interval, and the total integral is obtained by summation.

$$U(s,p) = (1+Ph_{\mathrm{I}})\sum_{n=1}^{N}\frac{\mathrm{d}S}{\mathrm{d}p}(p_n)\int_{p_{n-1}}^{p_n} G_{\xi=S(\tau)}\,\mathrm{d}\tau - \sum_{n=1}^{N}\int_{p_{n-1}}^{p_n}\left(\frac{\partial G}{\partial \xi}\right)_{\xi=S(\tau)}\mathrm{d}\tau \quad \text{for } s < S \qquad (43\text{a})$$

$$\frac{1}{2} = (1+Ph_{\mathrm{I}})\sum_{n=1}^{N}\frac{\mathrm{d}S}{\mathrm{d}p}(p_n)\int_{p_{n-1}}^{p_n} G_{\xi=S(\tau)}\,\mathrm{d}\tau - \sum_{n=1}^{N}\int_{p_{n-1}}^{p_n}\left(\frac{\partial G}{\partial \xi}\right)_{\xi=S(\tau)}\mathrm{d}\tau \quad \text{for } s = S \qquad (43\text{b})$$

with

$$\int G_{\xi=S(\tau)}\,\mathrm{d}\tau = \frac{H}{8}[\operatorname{erf} z_1 + e^{v_1}\operatorname{erf} z_2 - \operatorname{erf} z_3 - e^{v_2}\operatorname{erf} z_4] \qquad (44\text{a})$$

$$\int \frac{\partial G}{\partial \xi}_{\xi=S(\tau)}\,\mathrm{d}\tau = \frac{1}{2}[e^{v_1}\operatorname{erf} z_2 - e^{v_2}\operatorname{erf} z_4]. \qquad (44\text{b})$$

Boundary condition at s = 0 *of the second kind*: The equations resulting from (40a) and (40b) are

$$U(s,p) = \lim_{\varepsilon\to 0}\Bigg[Ph_{\mathrm{II}}\int_0^{p-\varepsilon}\left(G\frac{\mathrm{d}S}{\mathrm{d}p}\right)_{\xi=S(\tau)}\mathrm{d}\tau - \int_0^{p-\varepsilon} G_{\xi=0}\,\mathrm{d}\tau\Bigg] \quad \text{for } s < S \qquad (45\text{a})$$

$$0 = \lim_{\varepsilon\to 0}\Bigg[Ph_{\mathrm{II}}\int_0^{p-\varepsilon}\left(G\frac{\mathrm{d}S}{\mathrm{d}p}\right)_{\xi=S(\tau)}\mathrm{d}\tau - \int_0^{p-\varepsilon} G_{\xi=0}\,\mathrm{d}\tau\Bigg] \quad \text{for } s = S \qquad (45\text{b})$$

with the numerical forms

$$U(s,p) = Ph_{\mathrm{II}}\sum_{n=1}^{N}\frac{\mathrm{d}S}{\mathrm{d}p}(p_n)\int_{p_{n-1}}^{p_n} G_{\xi=S(\tau)}\,\mathrm{d}\tau - \int_0^{p-\varepsilon} G_{\xi=0}\,\mathrm{d}\tau \quad \text{for } s < S \qquad (46\text{a})$$

$$0 = Ph_{\mathrm{II}}\sum_{n=1}^{N}\frac{\mathrm{d}S}{\mathrm{d}p}(p_n)\int_{p_{n-1}}^{p_n} G_{\xi=S(\tau)}\,\mathrm{d}\tau - \int_0^{p-\varepsilon} G_{\xi=0}\,\mathrm{d}\tau \quad \text{for } s = S. \qquad (46\text{b})$$

The analytical solutions for the integrals are

$$\int G_{\xi=S(\tau)}\,\mathrm{d}\tau = -\frac{H}{8}[\operatorname{erf} z_1 + e^{v_1}\operatorname{erf} z_2 + \operatorname{erf} z_3 + e^{v_2}\operatorname{erf} z_4] \qquad (47\text{a})$$

$$\int G_{\xi=0}\,\mathrm{d}\tau = -\frac{y}{\sqrt{\pi}}c^{-\left(\frac{s}{y}\right)^2} - s\,\mathrm{erf}\left(\frac{s}{y}\right). \tag{47b}$$

Boundary condition at s = 0 *of the third kind*: The equations resulting from (40a), (40b) are the same as for the boundary condition of the first kind except that G from equation (30) is replaced by G from equation (32), and Ph_{I} by Ph_{III}. The analytical solutions of the integrals are

$$\int G_{\xi=S(\tau)}\,\mathrm{d}\tau = -\frac{H}{8}[\mathrm{erf}\,z_1 + e^{v_1}\,\mathrm{erf}\,z_2 + \mathrm{erf}\,z_3 + e^{v_2}\,\mathrm{erf}\,z_4]$$
$$+\frac{be^{v_3}}{v_4}e^{v_5}[1-\mathrm{erf}\,z_5] + \frac{H}{4v_4}[\mathrm{erf}\,z_1 + e^{v_1}\,\mathrm{erf}\,z_2] - \frac{b}{v_4}\mathrm{erf}\,z_1 \tag{48a}$$

$$\int \frac{\partial G}{\partial \xi}_{\xi=S(\tau)}\,\mathrm{d}\tau = -\frac{1}{2}[e^{v_1}\,\mathrm{erf}\,z_2 + e^{v_2}\,\mathrm{erf}\,z_4]$$
$$+\frac{e^{v_3}}{v_4}e^{v_5}[1-\mathrm{erf}\,z_5] + \frac{e^{v_1}}{v_4}\mathrm{erf}\,z_2. \tag{48b}$$

The meanings of z_1, z_2, z_3, z_4, etc. are explained in Table 1.

The iteration is carried out for each n, starting with $n = 1$, till the equation (43b) or (46b), respectively, is fulfilled within a required accuracy. Then $\mathrm{d}S/\mathrm{d}p$ and S are determined stepwise for the following n's till the solidification is complete at $S = 1$. With the known rate law $\mathrm{d}S/\mathrm{d}p$ [or $S(p)$] the temperature profile $U(s,p)$ can be computed using equation (43a), or (46a), respectively.

5. Analytical solutions

Before presenting the computational results obtained with the Green's function technique some analytical solutions will be discussed or derived, respectively, which will be used for comparison. It has been mentioned in the introduction that the only available exact analytical solution of the heat flow equation (1) refers to the boundary condition at $x = 0$ of the first kind, equation (5a), yielding the square root law $x_s = 2\eta_s\sqrt{at}$ for the growth of the solid shell (Neumann's solution). For the boundary condition of the second and third kind several approximate solutions can be derived. In the context of the present work we treat the so-called steady-state state solutions.

Neumann's solution (*boundary condition at* x = 0 *of the first kind*): For constant temperature at $x = 0$ the temperature distribution in the shell and the rate law of shell growth are given as

$$T = T_0 + \left[\frac{T_f - T_0}{\mathrm{erf}\,\eta_s}\right]\mathrm{erf}\left(\frac{x}{2\sqrt{at}}\right) \tag{49}$$

$$x_s = 2\eta_s\sqrt{at} \tag{50}$$

Table 1
Meanings of abbreviations used in equations (44), (47), (48)

$$V_n = \frac{S_n - S_{n-1}}{p_n - p_{n-1}}$$
$$H = \frac{4}{V_n}$$
$$A = -V_n(p-p_{n-1}) - S_{n-1} - S$$
$$B = -V_n(p-p_{n-1}) - S_{n-1} + S$$
$$y = \sqrt{4(p-\tau)}$$
$$z_1 = \frac{y}{H} + \frac{A}{y}$$
$$z_2 = \frac{y}{H} - \frac{A}{y}$$
$$z_3 = \frac{y}{H} + \frac{B}{y}$$
$$z_4 = \frac{y}{H} - \frac{B}{y}$$
$$z_5 = -z_1 + \frac{y}{2b} \quad \text{with}\, b = \frac{1}{Bi}$$
$$v_1 = -\frac{4A}{H}$$
$$v_2 = -\frac{4B}{H}$$
$$v_3 = -\frac{A}{b}$$
$$v_4 = 1 - \frac{4b}{H}$$
$$v_5 = \frac{y^2\left(1-\frac{4b}{H}\right)}{4b^2}$$

or in non-dimensional form, applying equations (6)–(9), as

$$U = \frac{\mathrm{erf}\left(\frac{s}{2\sqrt{p}}\right)}{\mathrm{erf}\,\eta_s} \tag{51}$$

with

$$S = 2\eta_s\sqrt{p}. \tag{52}$$

The rate constant η_s is related to the phase transformation number Ph_{I}, equation (15), by

$$\sqrt{\pi}\eta_s e^{\eta_s^2}\,\mathrm{erf}\,\eta_s = \frac{1}{Ph_{\mathrm{I}}}. \tag{53}$$

Steady-state solutions: The steady-state solutions of the heat flow equation (1) are obtained by setting the LHS in (1) equal to zero. This means that $\partial^2 T/\partial x^2$ is zero yielding the linear temperature profile in the shell

$$T = A + Bx. \tag{54}$$

The constants A and B are determined from the boundary condition at $x = 0$ and the boundary condition $T = T_f$ at $x = x_s$. The rate law of shell growth $x_s(t)$ is then determined from the condition (4).

Boundary condition at $x = 0$ *of the second kind*: For the boundary condition (5b) the coefficients A and B become

$$A = T_f - \frac{q_0 x_s}{\lambda} \tag{55a}$$

$$B = \frac{q_0}{\lambda}. \tag{55b}$$

The condition (4) yields

$$\frac{dx_s}{dt} = \frac{q_0}{\Delta H_f \rho} \tag{56}$$

and, after integration,

$$x_s = \frac{q_0}{\Delta H_f \rho} t. \tag{57}$$

Hence, the linear time-law for shell growth is obtained. Using the dimensionless quantities (7)–(9), (16), (21), the non-dimensional temperature profile and the growth law become

$$U = s - S \tag{58}$$

$$S = \frac{p}{Ph_{II}}. \tag{59}$$

The steady-state approximation should be approached when the capacitive property of the shell is small ($c_p \partial T/\partial t \to 0$). This is so when c_p is small or when the temperature stays close to T_f throughout the shell during the whole time of solidification. The latter is the case if q_0 and L are small and λ is large. Non-dimensionally, Ph_{II} should be large. Hence, the approximate solution should approach to the exact solution at large values of Ph_{II}.

Boundary condition at $x = 0$ *of the third kind*: For the boundary condition (5c) the coefficients A and B become

$$A = \frac{\lambda T_f + h T_w x_s}{\lambda + h x_s} \tag{60a}$$

$$B = \frac{h(T_f - T_w)}{\lambda + h x_s}. \tag{60b}$$

The condition (4) yields

$$\frac{dx_s}{dt} = \frac{\lambda h (T_f - T_w)}{\rho \Delta H_f (\lambda + h x_s)} \tag{61}$$

and, after integration,

$$x_s = \sqrt{\left(\frac{\lambda}{h}\right)^2 + \frac{2\lambda (T_f - T_w) t}{\rho \Delta H_f}} - \frac{\lambda}{h}. \tag{62}$$

Using the dimensionless quantities (7)–(9), (22), (27), (28) the dimensionless temperature profile and shell thickness become

$$U = \frac{1 + s\,Bi}{1 + S\,Bi} \tag{63}$$

$$S = \sqrt{\frac{1}{Bi^2} + \frac{2p}{Ph_{III}}} - \frac{1}{Bi}. \tag{64}$$

By the same reasoning as put forward in the previous paragraph with respect to the boundary condition of the second kind this approximate solution should approach to the exact solution at large Ph_{III} and small Bi.

6. Computational results

The equations (43), (46) were applied to compute the growth $S(p)$, of the shell and corresponding change of surface temperature $U_0(p)$ (for boundary condition at

Table 2
Material properties of iron and typical ranges for Ph and Bi

ΔH_f [J kg^{-1}]	247 000	
	(262 000	with heat of δ/γ transformation)
T_f [K]	1809	
$\bar{c}_p$* [J kg^{-1} K^{-1}]	750	for $T_0 > 1000$ K
λ [W K^{-1} m^{-1}]	32	for $T_0 > 1000$ K
a [m^2 s^{-1}]	$5.7 \cdot 10^{-6}$	for $T_0 > 1000$ K
Ph_I	0.4–1.2	in metal mold
Ph_{II}	0.08–0.12	in a continuous casting mold at a casting rate of 1 m min^{-1}
Ph_{III}	0.23	in the secondary cooling zone of continuous casting machine, depending on water flow rate
Bi	0.1–10	

* Average of c_p for solid iron in temperature range between T_f and T_0 computed from enthalpies H of solid iron as $\bar{c}_p = [H(T_f) - H(T_0)]/(T_f - T_0)$.

$s = 0$ of the second and third kind), for selected values of phase transformation number Ph_{I}, Ph_{II}, or phase transformation number Ph_{III} and Biot number Bi, respectively. The material properties of iron and the typical ranges for Ph and Bi in industrial casting processes are indicated in Table 2. The rate law $S/\sqrt{p}$ and the surface temperature $U_0(p)$ were then correlated with suitable combinations of phase transformation number, and Biot number, and dimensionless time. The results can readily be applied to obtain also the total solidification time p_{E} and surface temperature $U_0(p_{\mathrm{E}})$ at the end of solidification by setting $S = 1$.

Boundary condition at s = 0 *of the first kind*: Figure 3 shows, as an example, the shell thickness S as a function of time p for $Ph_{\mathrm{I}} = 0.5$. The numerically computed curve clearly is according to the square root law, $S \sim \sqrt{p}$, as required. Figure 4 gives the relationship between $S/\sqrt{p}$ and Ph_{I}. There is very good agreement with Neumann's solution, equation (53), which is included in Fig. 4 in the form of the dashed curve.

Boundary condition at s = 0 *of the second kind*: Two examples for the dependence of shell thickness S and surface temperature U_0 on time p are given in Fig. 5. For large values of Ph_{II}, S and U_0 vary almost linearly with p, Fig. 5(a), in close agreement with the steady-state approximation. But at small Ph_{II}, S and U_0 increase less than linearly with time, Fig. 5(b). It can be shown by dimensional analysis that $S/\sqrt{p}$ and $U_0/\sqrt{p}$ are unique functions of $\sqrt{p}/Ph_{\mathrm{II}}$. Alternatively, $S/\sqrt{p}$ and U_0/S can be given also as functions of S/Ph_{II}. Both types of relationships are presented in Fig. 6. The first, Fig. 6(a), is applied if S and U_0 are to be deduced as functions of p, and the second, Fig. 6(b), if p and U_0 are to be determined as functions of S. To facilitate the use of these correlations the following approximation formulae have been deduced for $\sqrt{p}/S$ and $-\sqrt{p}/U_0$ to represent the

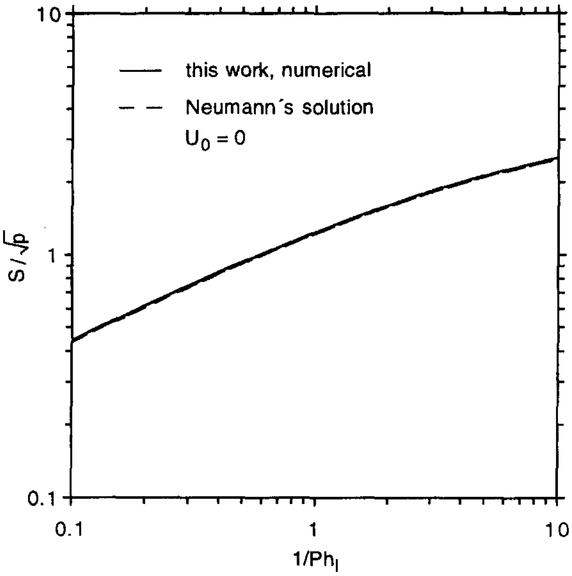

Fig. 4. Dimensionless rate constant $S/\sqrt{p}$ as a function of phase transformation number Ph_{I}. Boundary condition at $s = 0$ of the first kind. Comparison with Neumann's solution.

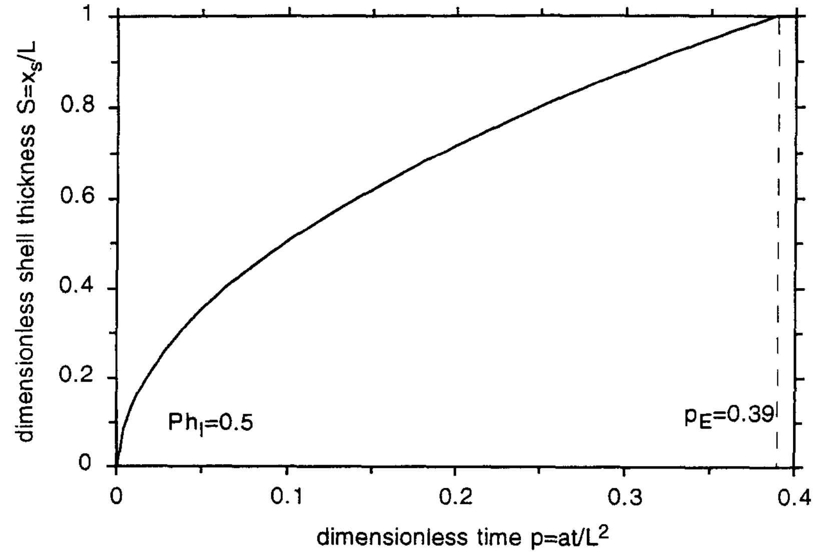

Fig. 3. Dimensionless shell thickness S as a function of dimensionless time p for a selected value of Ph_{I}. Numerical computation for boundary condition at $s = 0$ of the first kind.

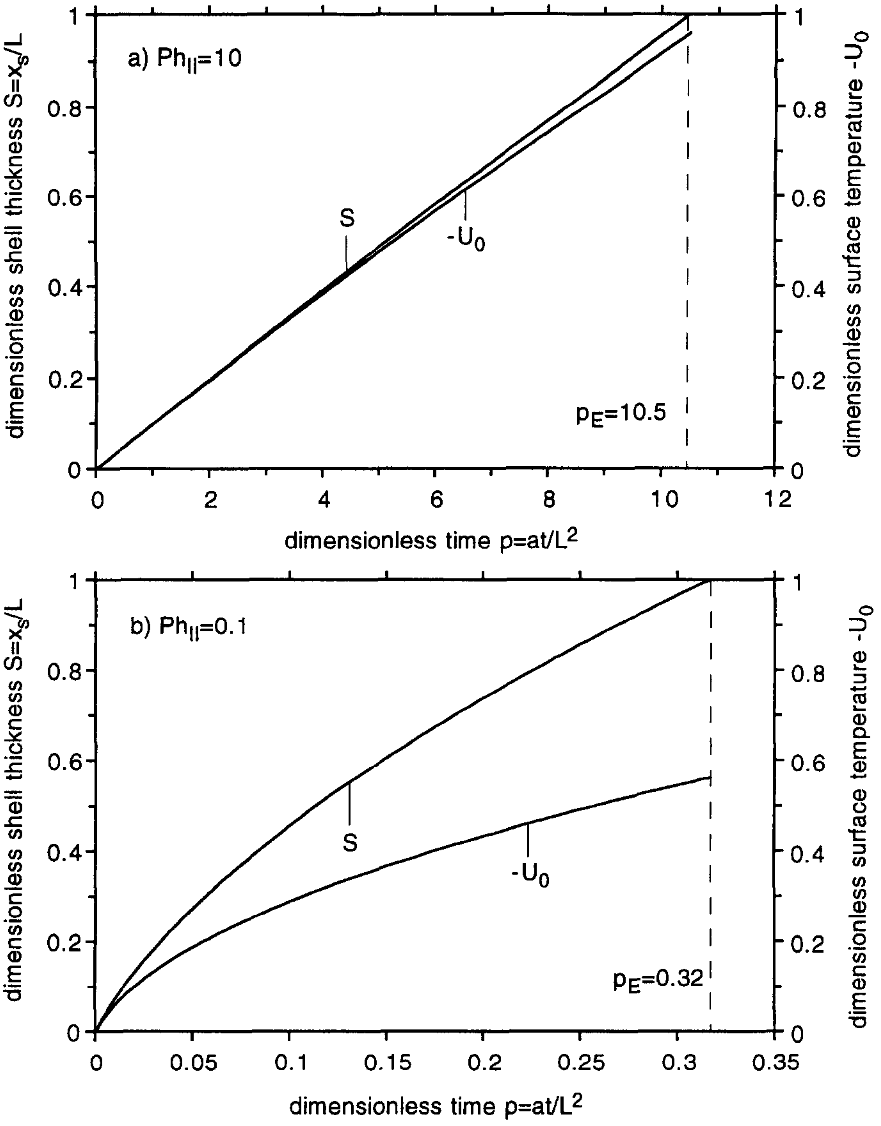

Fig. 5. Dimensionless shell thickness S and surface temperature U_0 as a function of dimensionless time p for two selected values of Ph_{II}. Boundary condition at $s = 0$ of the second kind. (a) $Ph_{II} = 10$, (b) $Ph_{II} = 0.1$.

numerically computed values, in the range $\sqrt{p}/Ph_{II} \leqslant 10$

$$\frac{\sqrt{p}}{S} = \frac{Ph_{II}}{\sqrt{p}} + 0.377\left(1 - e^{-1.49\frac{\sqrt{p}}{Ph_{II}}}\right) \tag{65}$$

$$-\frac{\sqrt{p}}{U_0} = \frac{Ph_{II}}{\sqrt{p}} + 0.84\left(1 - e^{-\frac{\sqrt{p}}{Ph_{II}}}\right). \tag{66}$$

Boundary condition at $s = 0$ *of the third kind*: For this boundary condition the $S-p$ and U_0-p curves depend on the two variables: Ph_{III} and Bi. Two examples are given in Fig. 7. At large Bi ($Bi \to \infty$) the boundary condition of the third kind reduces to that of the first kind, that is the surface temperature U_0 becomes constant and equal to zero ($T_0 = T_w$), and Neumann's solution is obeyed with the square root law $S = 2\eta_s\sqrt{p}$. This behavior is approached by the numerical solution for $Ph_{III} = 0.2$ and $Bi = 10$, Fig. 7(a). At small values of Bi the numerical solution yields a linear $S-p$ dependence, Fig. 7(b). It can be shown that for the boundary condition

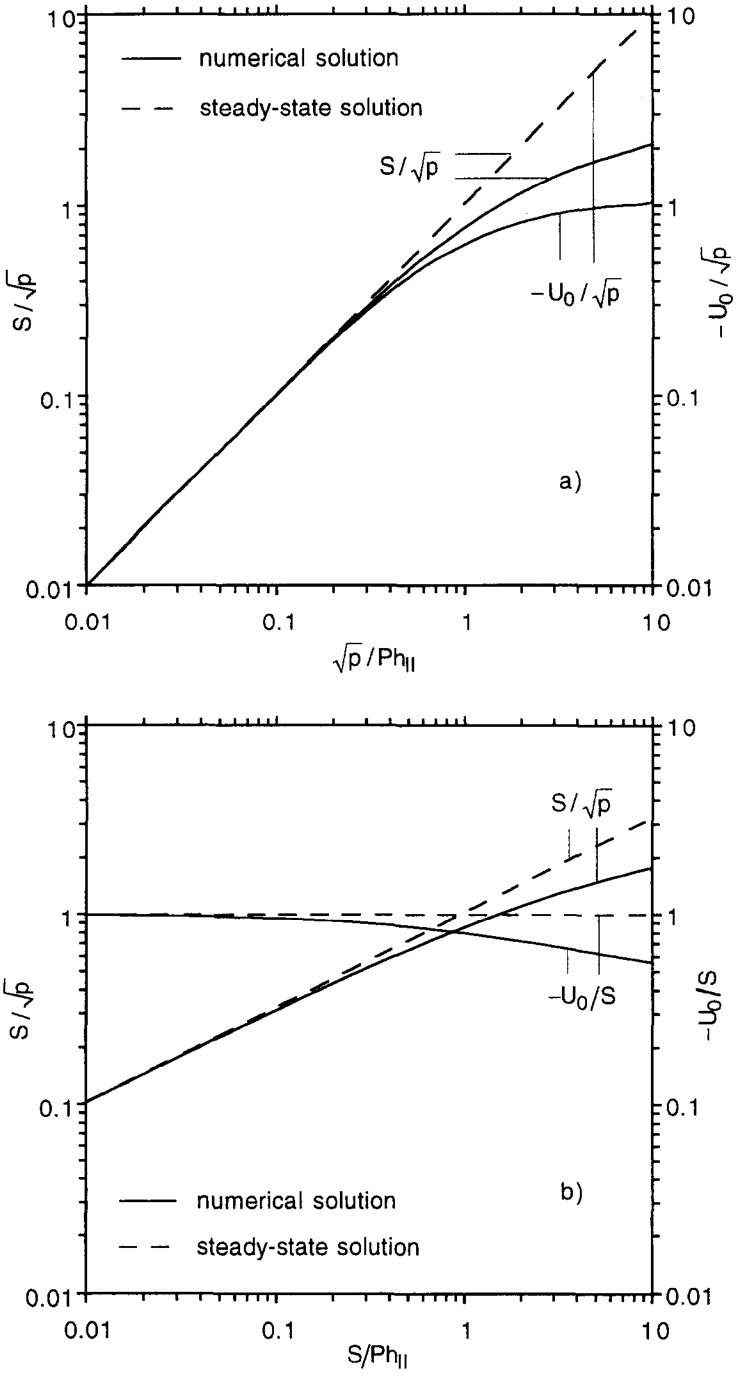

Fig. 6. Dimensionless correlations for the shell thickness S and surface temperature U_0. Boundary condition at $s = 0$ of the second kind. Comparison with steady-state solution.

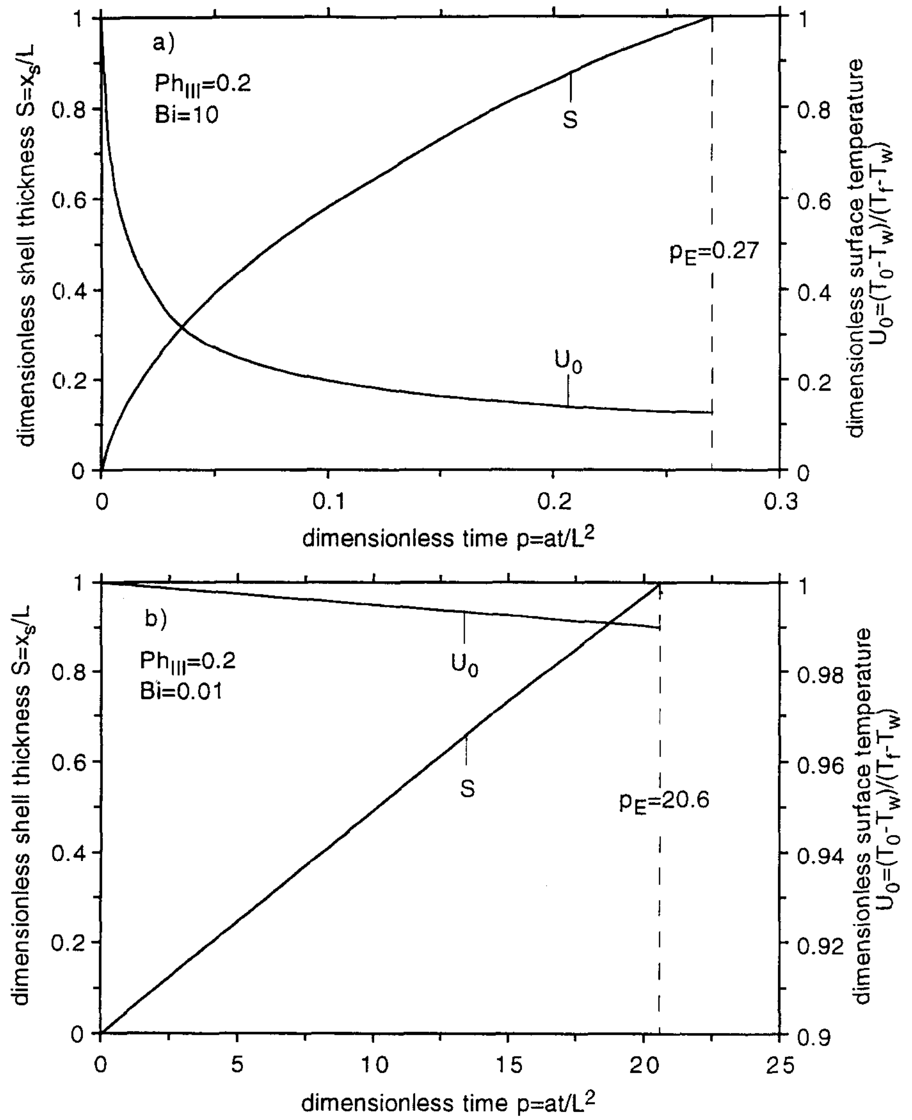

Fig. 7. Dimensionless shell thickness S and surface temperature U_0 as a function of dimensionless time p for two selected values of Bi at $Ph_{III} = 0.2$. Boundary condition at $s = 0$ of the third kind. (a) $Ph_{III} = 0.2$, $Bi = 10$, (b) $Ph_{III} = 0.2$, $Bi = 0.01$.

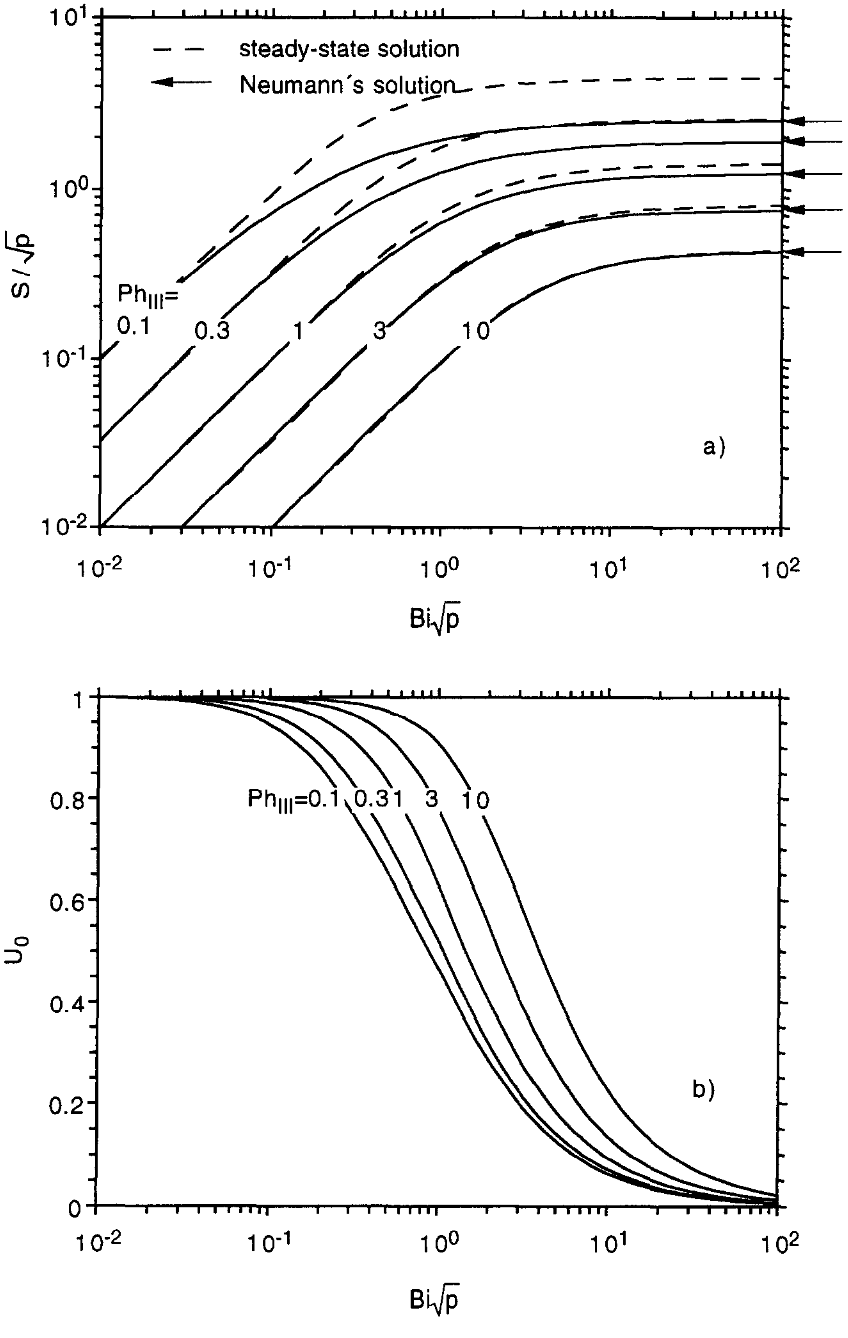

Fig. 8. Dimensionless correlations for shell thickness S and surface temperature U_0. Boundary condition at $s = 0$ of the third kind. Comparison with steady-state solution and Neumann's solution.

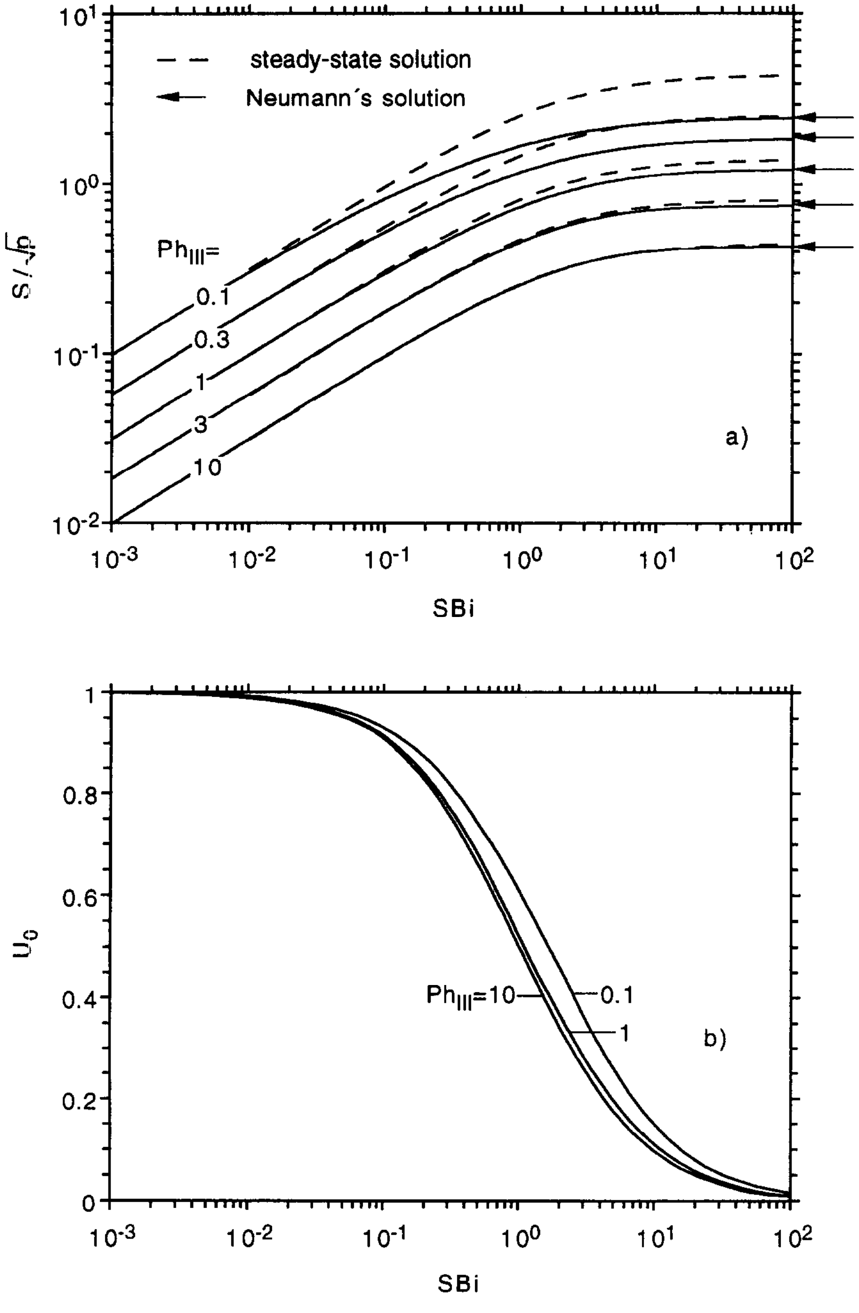

Fig. 9. Dimensionless correlations for shell thickness S and surface temperature U_0. Boundary condition at $s = 0$ of the third kind. Comparison with steady-state solution and Neumann's solution.

of the third kind $S/\sqrt{p}$ and U_0 are unique functions of $Bi\sqrt{p}$, at constant value of Ph_{III}. Alternatively, $S/\sqrt{p}$ and U_0 can be given also as functions of $S\,Bi$. The obtained correlations are shown in Figs. 8 and 9. The dashed lines in Figs. 8(a) and 9(a) represent the steady-state approximation which is approached at high Ph_{III} and small Bi as required. The following approximation formulae represent the numerically computed correlations in the range $Bi\sqrt{p} \leqslant 100$ and $Ph_{\mathrm{III}} \geqslant 0.1$

$$\frac{\sqrt{p}}{S} = \frac{Ph_{\mathrm{III}}}{Bi\sqrt{p}} + \frac{1}{2\eta_s}\left(1 - e^{-(0.53+0.50Ph_{\mathrm{III}}^{-1.34})(\sqrt{Bi\sqrt{p}})}\right) \tag{67}$$

$$\frac{1}{U_0} = \sqrt{1 + \frac{2Bi^2 p}{Ph_{\mathrm{III}}}} - \frac{0.35Ph_{\mathrm{III}}^{-1.64}(Bi\sqrt{p})^{2.5}}{1 + 0.50(1 + Ph_{\mathrm{III}}^{-0.98})(Bi\sqrt{p})^{1.5}}. \tag{68}$$

7. Summary and conclusion

In the present work the Green's function method has been applied to the solidification problem of pure materials, in plate geometry, involving the boundary conditions at the surface of the first, second, and third kind. In this method the heat flow equation is transformed, by application of a suitable Green's function, into an integral equation which is then solved numerically with a finite difference scheme. The advantage compared to the conventional numerical methods used to solve the heat flow equation, is a considerable decrease in computer time.

The results are presented in the form of dimensionless correlations for the shell thickness and surface temperature. These correlations can be utilized to predict the progress of solidification for a broad range of slab thickness, material properties, and cooling conditions. The numerical computations were compared with certain analytical solutions. The results for the boundary conditions at the surface of the first kind (T_0 = const) agree perfectly with the exact analytical solution by Neumann. The calculations for the boundary condition of the second (q_0 = const) and third kind (h = const) approach to the analytical solution for the steady-state behavior at high values of phase transformation number and low value of Biot number, as required.

References

[1] Chuang Y-K, Szekely J. On the use of Green's function for solving melting or solidification problems. Int J Heat Mass Transfer 1971;14:1285–94.

[2] Ehrich O, Chuang Y-K, Schwerdtfeger K. The melting of metal spheres involving the initially frozen shells with different material properties. Int J Heat Mass Transfer 1978;21:341–9.

[3] Chuang Y-K, Wepner W, Schwerdtfeger K. Berechnung der interdendritischen Anreicherung von Kohlenstoff und Sauerstoff bei der Erstarrung von Stahl. Arch Eisenhüttenwes 1973;44:243–50.

[4] Chuang Y-K, Ehrich O. On the integral technique for spherical growth problems. Int J Heat Mass Transfer 1974;17:945–53.

[5] Chuang Y-K, Szekely J. The use of Green's functions for solving melting or solidification problems in the cylindrical coordinate system. Int J Heat Mass Transfer 1972;15:1171–74.

[6] Carslaw HS, Jaeger JC. Conduction of Heat in Solids. Oxford: Oxford University Press, 1959.

[7] Bankoff SG. Heat conduction or diffusion with change of phase. Adv Chem Engng 1964;5:75–150.

[8] Sekerka RF. A Green's function to describe the time-dependent shape of a morphologically unstable solid–liquid interface during solidification. J Crystal Growth 1971;10:239–50.

[9] Budhia H, Kreith F. Heat transfer with melting or freezing in a wedge. Int J Heat Mass Transfer 1973;16:195–211.

[10] Liarokapis E, Raptis YS. Temperature rise induced by a cw laser beam revisited. J Appl Phys 1985;57(12):5123–26.